Eur Biophys J (1988) 15: 321–328

European Biophysics Journal

A laser-T-jump study of the adsorption of dipolar molecules to planar lipid membranes

II. Phloretin and phloretin analogues

R. Awiszus and G. Stark*

Fakultät für Biologie, Universität Konstanz, D-7750 Konstanz, Federal Republic of Germany

Received March 10, 1987/Accepted in revised form September 28, 1987

Abstract. Phloretin and structurally related neutral molecules adsorb to the interface of lipid membranes and modify the electric dipole potential of the membrane/water interface. The adsorption process has been studied using a laser-T-jump relaxation technique in combination with an analysis of nonactin mediated potassium transport (see part I, Awiszus and Stark 1988).

Deviations from the Langmuir isotherm were observed for most of the substances. The discrepancies were most pronounced at large surface densities, whereas good agreement was found at low concentrations in many cases.

The partition coefficient in the limit of low concentrations was compared with that of octanol/water bulk phases. No correlation was found. The individual values of the two partition coefficients differed by more than three orders of magnitude. The contribution, b, of a single adsorbed molecule to the dipole potential could not be predicted from the dipole moment, μ_L, of the molecule measured in the bulk phase. Different values of b were found at identical values of μ_L.

The study shows the limitations of the use of bulk phase data to predict molecular properties in lipid membranes.

Key words: Adsorption, lipid membranes, laser-T-jump, Langmuir isotherm, phloretin

Introduction

The adsorption of phloretin to biological membranes was found to influence the transport of many different species, both electrolytes and non-electrolytes. In the human red blood cell inhibition of hexose (Le Fevre 1961) and chloride transport (Wieth et al. 1973) was observed, as well as a lowering of the permeability to glycerol and urea (Macey and Farmer 1970). Similar effects were found with other biological membranes. Andersen et al. (1976) and Melnik et al. (1977) tried to find a general physicochemical mechanism for the diversity of phloretin effects on membrane transport. They reported a marked change of the potential difference between the membrane interior and water (dipole potential). This is a consequence of the oriented adsorption of molecules with a large dipole moment to the membrane/water interface. Following the adsorption of phloretin to artificial lipid membranes, a marked increase of the membrane conductance in the presence of lipophilic cations or in the presence of carrier mediated cation transport, and a concomitant decrease of lipophilic anion conductivity is observed. The effect may be used to estimate the magnitude of the dipole potential (McLaughlin 1973). This was performed in the case of phloretin by DeLevie et al. (1979).

Phloretin binding as a function of the aqueous concentration was found to obey Langmuir's isotherm. This was concluded indirectly from the concentration dependence of the dipole potential measured at planar lipid membranes (DeLevie et al. 1979). Spectrophotometric studies (Verkman and Solomon 1980) and fluorescence quenching techniques (Verkman 1980) at lipid vesicles were also interpreted on the basis of this isotherm.

There is a twofold goal of our present studies. For the first time we determine the interfacial concentration of phloretin as a function of the aqueous concentration at planar lipid membranes and we correlate our results with an analysis of the effect of phloretin on carrier mediated ion transport. This is done by applying the procedure outlined in part I of this series (Awiszus and Stark 1988). As a result the contribution of a single adsorbed phloretin molecule to the interfacial dipole potential is obtained. Secondly the procedure is applied to a series of structurally related analogues of phloretin, which are compared with respect to their dipolar properties and their binding behaviour.

* To whom offprint requests should be sent

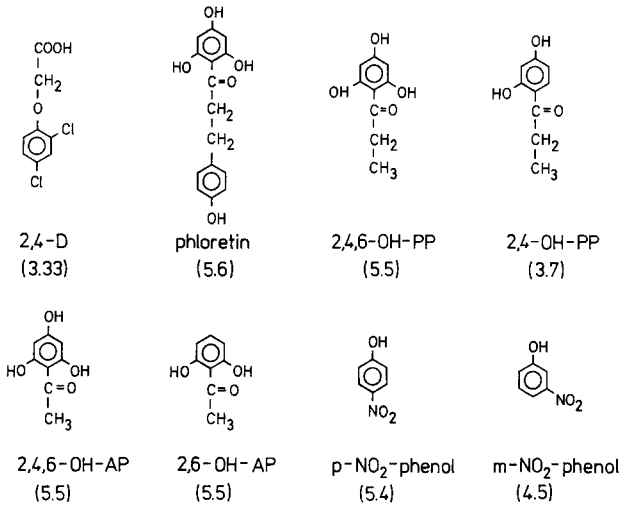

Fig. 1. Chemical structure of the molecules investigated: 2,4-dichlorophenoxyacetic acid (2,4-D); 2′,4′,6′-trihydroxy-3-(*p*-hydroxyphenyl)propiophenone (phloretin); 2′,4′,6′-trihydroxypropiophenone (2,4,6-OH-PP); 2′,4′-dihydroxypropiophenone (2,4-OH-PP); 2′,4′,6′-trihydroxyacetophenone (2,4,6-OH-AP); 2′,6′-dihydroxyacetophenone (2,6-OH-AP). The numbers in brackets represent dipole moments in Debye units (1 D = $3.34 \cdot 10^{-30}$ Asm) taken from Andersen et al. (1976) and Reyes et al. (1983)

Finally, the limitations of Langmuir's isotherm, as applied to the problem under investigation, will become apparent.

Experimental

The structure of the molecules which were used is shown in Fig. 1. Phloretin was obtained from Sigma, all the other substances from Aldrich Chemical Co. They showed a single spot in thin layer chromatography and were used without further purification. The pK-values of all substances are greater than 7 (Reyes et al. 1983). Since the experiments were performed at pH 4 (pH 5 in the case of phloretin), the compounds were almost completely in the protonated (neutral) form. Stock solutions in ethanol (phloretin and 2,4,6-OH-PP) or DMSO (all other substances) were used to prepare the aqueous solutions. The amount of organic solvent in the latter was always less than 1% (w/v). Further experimental details were identical to those described in part I (Awiszus and Stark 1988).

Results and discussions

The adsorption of the dipolar molecules shown in Fig. 1 was studied via their influence on potassium transport mediated by the macrocyclic ion carrier nonactin. The procedure, including the applied model with its assumptions and the theoretical treatment,

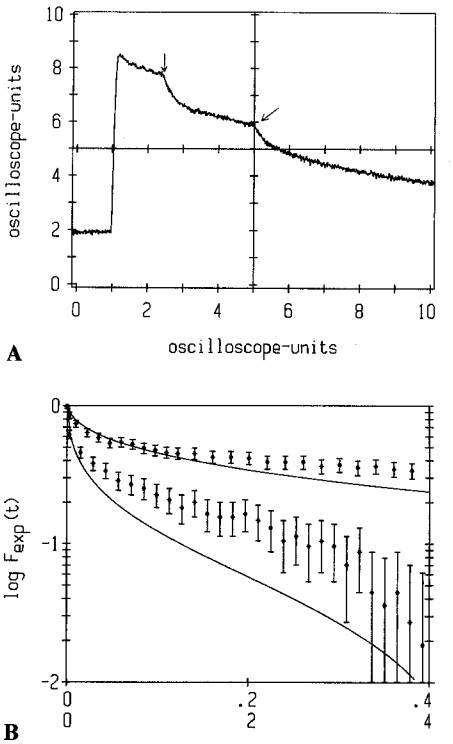

Fig. 2 A and B. T-jump induced current relaxation observed in the presence of phloretin and nonactin. Aqueous solution: 0.1 *M* KCl, 0.9 *M* LiCl, 10 m*M* acetate buffer (pH 5), 10^{-7} *M* nonactin and $4 \cdot 10^{-5}$ *M* phloretin. Membrane area 0.02 cm^2, applied voltage 50 mV, membrane conductance $6.7 \cdot 10^{-3}$ S cm^{-2}. **A** record of the current transient. Oscilloscope: Vertical sensitivity 10 nA/division, the time scale was changed at the indicated *arrows* from 2 ms/division to 50 ms/division and finally to 1 s/division. **B** Analysis of the data according to Eq. (19) of Awiszus and Stark (1988) using two different time scales. The *solid lines* were calculated from Eqs. (15) and (20) with $t_1 = 400\,\mu s$, $t_2 = 4.5$ s, $D = 5.5 \cdot 10^{-6}$ cm^2/s and $\beta^* = 9.04 \cdot 10^{-4}$ cm

was outlined in detail in part I (Awiszus and Stark 1988).

In brief, the adsorption modifies the rate constants of the carrier transport and, as a consequence, the membrane conductance. The dynamics of adsorption is measured via a temperature-jump induced relaxation of the electric current: As the temperature is increased, the interfacial concentration, N, of adsorbed molecules is decreased, leading to a smaller membrane conductance. From the time course of the electric current, the effective partition coefficient, β^*, may be obtained. The analysis was performed on the basis of Langmuir's adsorption isotherm, assuming a fixed surface density, N_D, of binding sites and an aqueous concentration at half saturation of the sites, K_S ($K_S = N_D/\beta$, β = concentration independent partition coefficient at low surface densities). The measurement of β^* as a function of the bulk ligand concentration, C_B, allows one to estimate the model parameters β, K_S and N_D.

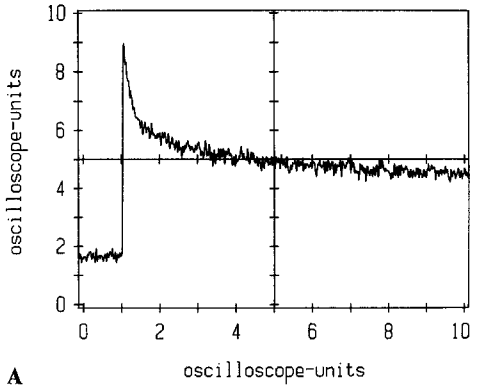

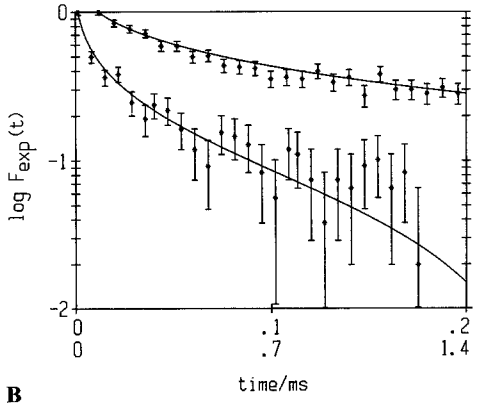

Fig. 3 A and B. T-jump induced current relaxation observed in the presence of *p*-nitrophenol and nonactin using the *Q*-switch mode of the laser. Aqueous solutions: 1 *M* KCl, 10 m*M* acetate buffer (pH 4), $5 \cdot 10^{-7}$ *M* nonactin and 10^{-3} *M* *p*-nitrophenol. Membrane area $5 \cdot 10^{-3}$ cm^2, applied voltage 50 mV, membrane conductance $1.2 \cdot 10^{-2}$ S cm^{-2}. **A** record of the current transient. Oscilloscope: Vertical sensitivity 5 nA/division, time scale 200 µs/division. **B** Analysis of the data according to Eq. (19) of Awiszus and Stark (1988) using two different time scales. The *solid lines* were calculated from Eqs. (15) and (20) with t_1 = 12 µs, t_2 = 16 ms, $D = 6.9 \cdot 10^{-6}$ cm^2/s and $\beta^* = 1.6 \cdot 10^{-5}$ cm. Using these values, $F(t_1) = 0.59$ and $F(t_2) = 0.083$ is obtained. The *error bars* indicate the measurement uncertainty

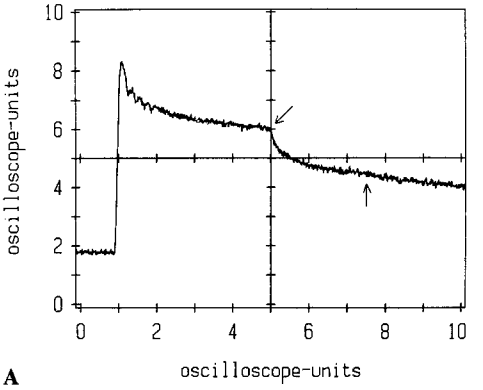

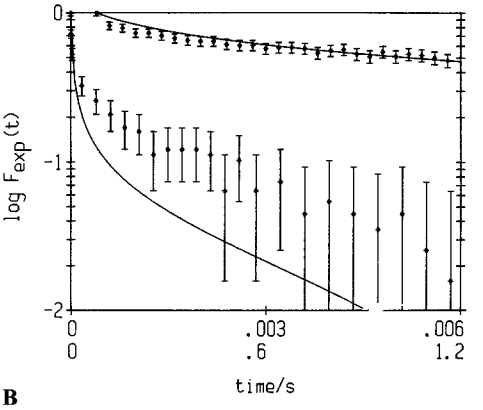

Fig. 4 A and B. T-jump induced current relaxation observed in the presence of *p*-nitrophenol and nonactin using the fixed Q-mode of the laser. Aqueous solutions: 1 *M* KCl, 10 m*M* acetate buffer (pH 4), $5 \cdot 10^{-8}$ *M* nonactin and 10^{-3} *M* *p*-nitrophenol. Membrane area 0.02 cm^2, applied voltage 50 mV, membrane conductance $5 \cdot 10^{-3}$ S cm^{-2}. **A** record of the current transient. Oscilloscope: Vertical sensitivity 10 nA/division, the time scale was changed at the indicated *arrows* from 2 ms/division to 200 ms/division and finally to 500 ms/division. **B** Analysis of the data according to Eq. (19) using two different time scales. The *solid lines* were calculated from Eqs. (15) and (20) with t_1 = 400 µs, t_2 = 1.4 s, $D = 6.9 \cdot 10^{-6}$ cm^2/s and $\beta^* = 1.5 \cdot 10^{-4}$ cm

Application of this procedure represents a test of the validity of Langmuir's equation for the problem under study. Both, the time course $F(t)$ of the relaxation and the dependence of β^* on the concentration, C_B, should agree with the relevant theoretical equations. For the herbicide 2,4-D good correspondence between theory and experiment was achieved (cf. part I). Deviations were found, however, with phloretin and with most of the other chemicals.

At small ligand concentrations, C_B, the quantity

$$F(t)_{exp} = (J(t) - J(t_2))/(J(t_1) - J(t_2))$$

($J(t)$ = electric current density, $t_1(t_2)$ = minimum (maximum) time of measurement) was in good agreement with the theory (exception see below). At large ligand concentrations, however, the data could not be fitted by the theoretical equations. This is illustrated for phloretin in Fig. 2. While the discrepancy between theory and experiment is apparent at a phloretin concentration of $4 \cdot 10^{-5}$ *M*, theory provides a reasonable description of the data at smaller concentrations (cf. Fig. 4 of part I). Similar behaviour was observed for 2,4,6-OH-PP and 2,4,6-OH-AP. Only for 2,4-OH-PP were theory and experiment in agreement at all concentrations studied (not shown). In contrast, disagreement over the whole concentration range was found for 2,6-OH-AP, para- and meta-nitrophenol. This is shown for *p*-nitrophenol in Figs. 3 and 4. The relaxation phenomena are faster in this case so that the *Q*-switch mode of the laser was used in addition to the fixed *Q*-mode normally applied. In the *Q*-switch mode the pulse width of the laser beam, and concomitantly the rise time of the T-jump, is reduced to about 40 ns.

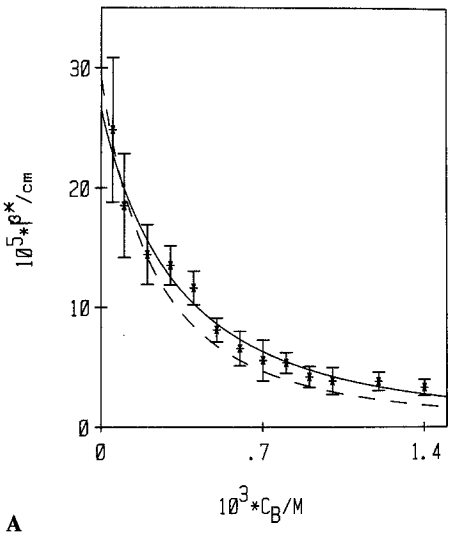

A

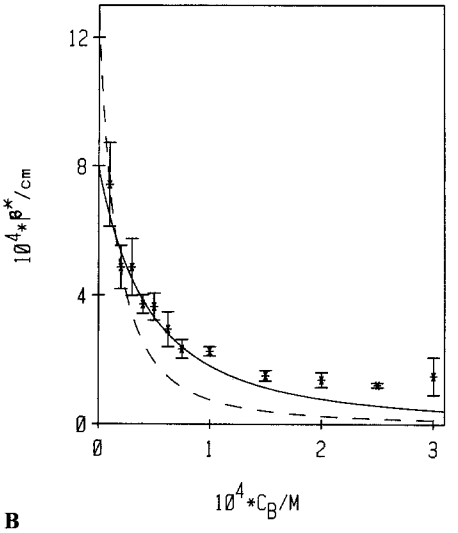

B

Fig. 5 A and B. The effective partition coefficient, β^*, as a function of the concentration, C_B, in water. The data points are mean values of at least 5 different measurements, the *bars* represent the standard deviation. The *solid* (*broken*) *lines* were calculated according to Eqs. (3) and (11) of Awiszus and Stark (1988) (values for the *broken lines* in brackets). **A** 2,4-OH-PP: *solid* (*broken*) *line* fitted to all (the first three) data points. $\beta = 2.64 \cdot 10^{-4}$ ($2.9 \cdot 10^{-4}$) cm, $N_D = 1.06 \cdot 10^{14}$ ($8.13 \cdot 10^{13}$) cm^{-2}. **B** 2,4,6-OH-PP: *solid* (*broken*) line fitted to seven (two) data points. $\beta = 7.9 \cdot 10^{-4}$ ($12.7 \cdot 10^{-4}$) cm, $N_D = 4.4 \cdot 10^{13}$ ($2.5 \cdot 10^{13}$) cm^{-2}

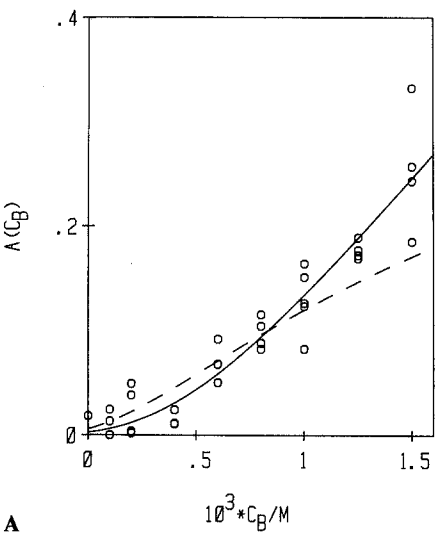

A

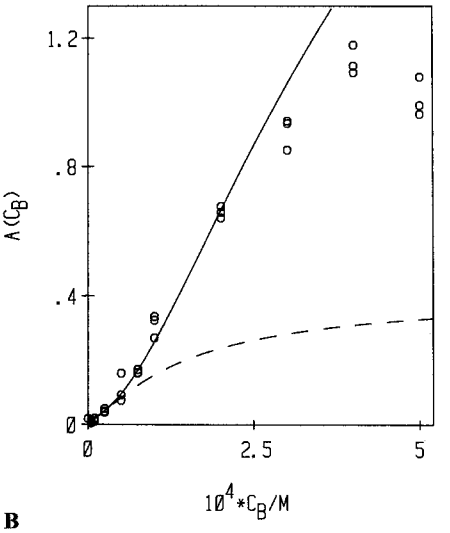

B

Fig. 6 A and B. The parameter A as a function of the bulk concentration, C_B. The data were obtained from single membranes except for $C_B = 0$ (mean value of 19 membranes). Eq. (31) in combination with Eq. (2) of Awiszus and Stark (1988) was fitted to the data. The following values of parameters were obtained (using $v_0 = 0$, values for the *broken line* in brackets): **A** 2,4-OH-PP: $z_0 = 1.3 \cdot 10^{-3}$ ($2.9 \cdot 10^{-3}$), $b(1-a) = 1.6 \cdot 10^{-15}$ ($1.4 \cdot 10^{-15}$) V cm^2, **B** 2,4,6-OH-PP: $z_0 = 6 \cdot 10^{-3}$ ($3.5 \cdot 10^{-3}$), $b(1-a) = 3.4 \cdot 10^{-15}$ ($4.2 \cdot 10^{-15}$) V cm^2. The values of β and N_D were taken as given in the legend to Fig. 5

The time resolution of the method, limited by the detection system of the membrane current, is about 10 µs in this case. The temperature stability after a T-jump is, however, reduced by about two orders of magnitude in time. This is the consequence of the comparatively small diameter of the laser beam (about 0.5 mm). While beam diameters of about 6–10 mm are used in the fixed Q-mode (depending on the membrane diameter), the diameter had to be reduced in the Q-switch mode in order to avoid signal distortion due to the presence of shock waves. To cover the whole time range of the relaxation, a combination of a Q-switch and a fixed Q-experiment was used (Figs. 3 and 4). While the theory adequately explained the fast part of the relaxation (up to the millisecond region), there are clear discrepancies at longer times. This was found at all concentrations of para- and meta-nitrophenol. In the presence of any of the other substances, both kinds of experiment (fixed Q or Q-switch) could be fitted with the same value of β^*.

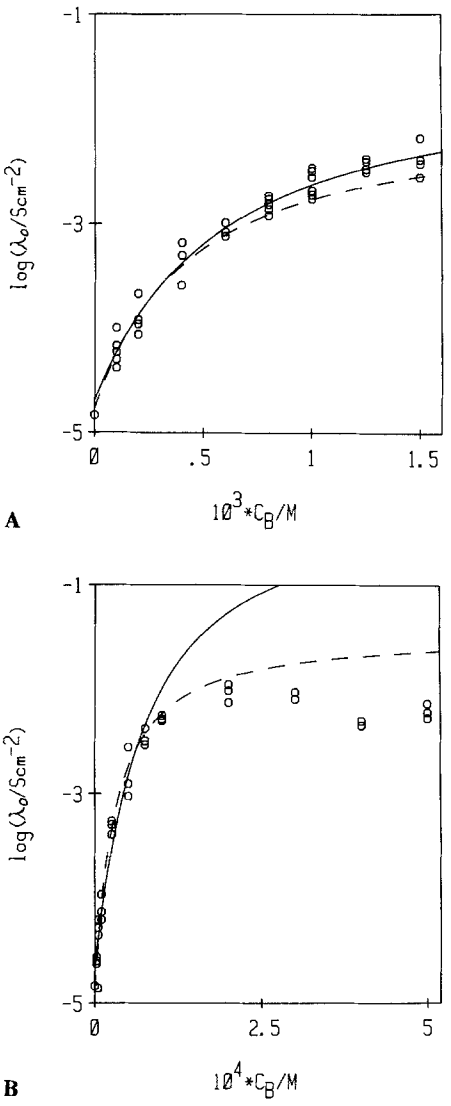

Fig. 7 A and B. Zero voltage conductance, λ_0, as a function of the bulk concentration, C_B. The data were obtained from single membranes except for $C_B = 0$ (mean value of 25 membranes). The *solid* (*broken*) *lines* represent a fit of Eqs. (30) and (31) of Awiszus and Stark (1988) to the data using values z_0 and $b(1-a)$ from the analysis of the current-voltage characteristic (cf. legend to Fig. 6). **A** 2,4-OH-PP: $E = 1 \cdot 10^{-6}$ $(8.5 \cdot 10^{-7})$ A cm^{-2}, $b = 2 \cdot 10^{-15}$ $(2.2 \cdot 10^{-15})$ V cm^2. **B** 2,4,6-OH-PP: $E = 1.2 \cdot 10^{-6}$ $(6.8 \cdot 10^{-7})$ A cm^{-2}, $b = 7.1 \cdot 10^{-15}$ $(8.5 \cdot 10^{-15})$ V cm^2

The theoretical analysis of $F(t)$ is based on the Langmuir isotherm. There may be several reasons for the discrepancies observed:

The shape of the adsorption isotherm might differ from that proposed by Langmuir. In the simplest case more than one class of identical binding sites could exist. In addition, the Langmuir isotherm neglects the interaction of adsorbed molecules. Such an interaction could give rise to a concentration-dependent contribution, b, of adsorbed molecules to the dipole potential, V_D. This may be imagined as follows: At small surface densities, N, the adsorbed molecules are independent. At high surface densities, the interaction between neighbouring molecules leads to a change of b; i.e., the angle of the dipole moment with the membrane/water interface becomes concentration dependent. Finally, the presence of impurities may become important at high aqueous concentration, C_B.

Thus far, there is no way to discriminate between the different effects on $F(t)$. In view of the observed discrepancies further analysis was restricted to phloretin, 2,4,6-OH-AP, 2,4-OH-PP and to 2,4,6-OH-PP, i.e., to those substances where agreement between theory and experiment was observed at least within the low concentration range. For 2,4-OH-PP, where $F(t)$ was found to fit at all applied concentrations, the same procedure was used as in the case of 2,4-D (cf. part I). For the three other substances, theory and experiments were compared in the low concentration range only. For 2,4-OH-PP and for 2,4,6-OH-PP the results are presented in detail (see Figs. 5–8). In the case of phloretin and 2,4,6-OH-AP, the analysis was performed in the same way as described below for 2,4,6-OH-PP. Finally, the data for all four compounds is summarized in Table 1.

For 2,4-OH-PP a reasonable fit of the data over the whole concentration range is obtained irrespective of whether the complete set of experimental data is used to determine the parameters of the applied model, or whether only the data at low concentrations are used (Figs. 5 A, 6 A, 7 A and 8 A). This is in agreement with the good fit of $F(t)$ observed at all concentrations. Thus, the applied model represents a satisfactory picture of the experimental reality for this substance.

For 2,4,6-OH-PP (as well as for 2,4,6-OH-AP and for phloretin) the fit in Figs. 5–8 was limited to the low concentration range, i.e., to the range of reliable values for the effective partition coefficient, β^*. At larger values of C_B, the data for β^* represent the best fit obtained for $k^* \to \infty$ (cf. Fig. 2). The fit was not improved at lower values of k^*. Extrapolation of the curves, adapted to the low concentration range, to the range of large concentrations shows clear discrepancies, if compared with the data (cf. Figs. 5 B, 6 B, 7 B and 8 B). This underlines the conclusion already reached in the study of the concentration dependence of $F(t)$: Additional effects, not included in the model used seem to influence the adsorption behaviour of these substances.

Consequently, the data summarized in Table 1 refer to the low concentration range. There, deviations from the ideal Langmuir behaviour can obviously be neglected. As far as the high concentration range is concerned (e.g., the maximum number N_D of adsorption sites) the values represent extrapolations, which differ in a unpredictable way from the true values. Only for 2,4-OH-PP do the data reliably reflect the

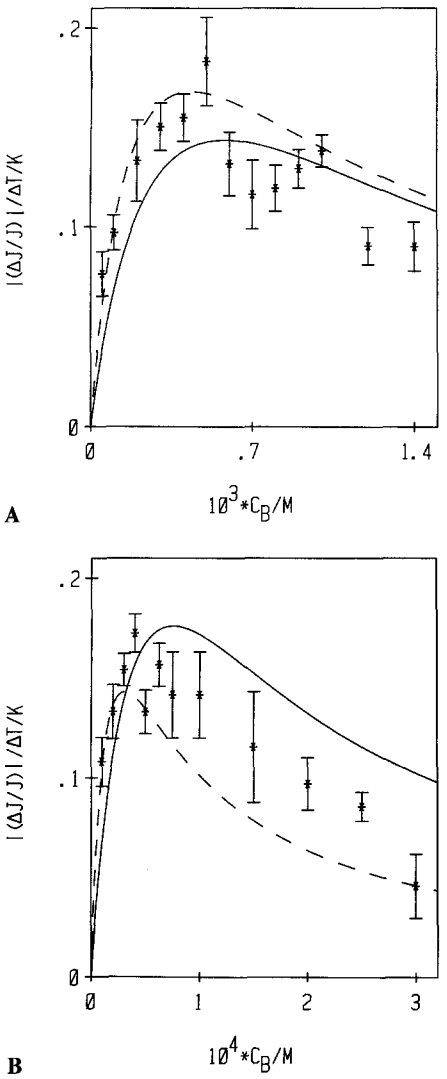

Fig. 8 A and B. The reduced relaxation amplitude $|\Delta J/J|/\Delta T$ as a function of the bulk concentration, C_B. The *solid (broken) line* was calculated according to Eq. (32) of Awiszus and Stark (1988) using values for the parameters given in Table 1. The only free parameter is $\Delta\beta/\Delta T$. **A** 2,4-OH-PP: $\Delta\beta/\Delta T = 2 \cdot 10^{-5}$ $(2.9 \cdot 10^{-5})$ cm/K; **B** 2,4,6-OH-PP: $\Delta\beta/\Delta T = 5.1 \cdot 10^{-5}$ $(9.1 \cdot 10^{-5})$ cm/K

experimental behaviour over the complete concentration range.

In spite of their limited reliability, the data in various respects extend our knowledge on the interfacial adsorption of the substances studied. To date only the aqueous concentration at half saturation of the binding sites, K_{HA}, as well as the maximum change, V_D^{max}, of the interfacial dipole potential has been known. Our data agree with those of Reyes et al. (1983), obtained for phosphatidylethanolamine bilayers, within a factor of 2. Verkman and Solomon (1980) studied the kinetics of adsorption of phloretin to unilamellar lipid vesicles using a conventional T-jump technique developed for homogeneous solutions. A dissociation constant, K_{HA}, of 8 μM and a lipid/site ratio of 4 was obtained. The last value corresponds to a maximum density of sites, N_D, of about $4 \cdot 10^{13}\,\mathrm{cm}^{-2}$, in approximate agreement with our data for planar bilayers. The authors were also able to measure the rate constant of desorption ($k_{HA} = 2900\,\mathrm{s}^{-1}$). This is the consequence of the three-dimensional (spherical) diffusion problem, which allows the determination of larger values as compared to the one-dimensional problem encountered at planar membranes. In the latter case unstirred layer diffusion permitted us to determine only the lower limit for k_{HA} ($k_{HA} \geqq 1\,\mathrm{s}^{-1}$ for phloretin).

The main advantage of the planar membrane system is the combination of kinetic and electric measurements. As a consequence, the contribution, b, of a single adsorbed molecule to the dipole potential was obtained. b depends on the dipole moment, μ, perpendicular to the membrane interface through adsorption of a single ligand molecule and on the dielectric constant, ε, within the adsorption layer ($b = \mu/\varepsilon\,\varepsilon_0$). μ includes contributions from the dipole moment, μ_L, of the ligand molecule as well as changes of the dipolar structure of the membrane/water interface which are induced through ligand adsorption. The effect of the latter (including contributions of oriented water molecules) cannot be neglected. This is apparent from

Table 1. Model parameters for the adsorption of phloretin and analogous substances to the membrane/water interface of dioleoyllecithin membranes (for a definition of the symbols see Awiszus and Stark 1988). The number in brackets refer to the broken lines in Figs. 5–8

	2,4,6-OH-AP	2,4-OH-PP	2,4,6-OH-PP	Phloretin
$10^4\,\beta_{HA}$/cm	5.4	2.6 (2.9)	7.9 (12.7)	45
$10^{-13}\,N_D$/cm^{-2}	4	10.6 (8.1)	4.4 (2.5)	2.2
$10^4\,K_{HA}/M$	1.2	6.7 (4.7)	0.9 (0.3)	0.08
$10^{15}\,b$/V cm^2	3.9	2 (2.2)	7.1 (8.5)	12.7
μ_L/Debye [a]	5.5	3.7	5.5	5.6
a	0.3	0.2 (0.36)	0.5 (0.5)	0.6
$\Delta H_0(\beta)$/kJ mol^{-1}	−84	−55 (−74)	−47 (−53)	−40
$10^6\,D$/cm^2 s^{-1} [b]	6.2	6.5	6.1	5.5

[a] taken from Andersen et al. (1976) and Reyes et al. (1983)

[b] estimated from experimental values of similar substance using Stoke's law. The data are necessary for the calculation of β^* (cf. Eqs. (9) and (10) of part I)

Table 2. Comparison between the partition coefficients of octanol/water ($\gamma_{o/w}$) and of the membrane/water interface of dioleoyllecithin membranes ($\gamma_{m/w}$)

	2,4,6-OH-AP	2,4-OH-PP	2,4,6-OH-PP	Phloretin	2,4-D
$\gamma_{m/w}$ [a]	2160	1040	3160	18000	1880
$\gamma_{o/w}$ [b]	1.2	12.6	4.2	–	646

[a] calculated from Table 1 ($\gamma_{m/w}$) = $2\beta_{HA}/d$, d = membrane thickness (50 Å))
[b] according to Cousin and Motais (1978) and Hansch and Leo (1979)

a comparison of b and μ_L (Table 1). While μ_L is largely identical for three of the four substance, b shows large differences. The data for μ_L represent weighted averages of the squares of the dipole moments of all molecular conformations. Thus, the differences in the behaviour of b as compared to μ_L might also be due to special conformations at the interface as well as to a different angle between μ_L and the membrane interface for the individual substances. In conclusion, the effect of ligand adsorption on the dipole potential cannot be predicted from the dipole moment measured in bulk solutions.

A similar conclusion holds for the partition coefficient (at low surface densities). Since the classical studies of Collander and Bärlund (1933), the partition coefficient of neutral substances between membrane and water is usually estimated via the oil/water partition coefficient (recently reviewed by Lieb and Stein 1986). There seems to be general agreement about a positive correlation between the two kinds of partition coefficients, if the average of many experimental values is considered. A comparison of the partition coefficients for individual substances may, however, show enormous differences. This is illustrated in Table 2. The dimensionless partition coefficient $\gamma_{m/w}$ (calculated from β_{HA}) is compared with the octanol/water coefficient $\gamma_{o/w}$. The values for the latter were either determined experimentally (Hansch and Leo 1979) or were calculated from experimental values of similar substances assuming well established values for substituents, such as OH-groups (Cousin and Motais 1978). While the values for 2,4-D agree within a factor of three, differences of more than three orders of magnitude are obtained in the case of 2,4,6-OH-AP. Differences are observed in the effect of an OH-substituent, too. $\gamma_{o/w}$ is larger for 2,4-OH-PP as compared to 2,4,6-OH-PP, i.e. the addition of an OH-group favours the concentration in water as compared to octanol. The opposite behaviour is found for $\gamma_{m/w}$.

The clear discrepancies obtained for the two partition coefficients may be interpreted as follows. In addition to the fundamental structural differences between a membrane/water-interface and a bulk phase, such as octanol, $\gamma_{m/w}$ is influenced through the electrostatic interaction between the dipole moment of the adsorbed ligand and the intrinsic dipole potential of the membrane/water-interface. The latter is of the order 100–300 mV (positive towards the membrane interior) depending on the kind of lipid. It is responsible for the enhanced membrane permeability of negatively charged hydrophobic ions as compared to positively charged ions (Liberman and Topaly 1969; Szabo 1976; Pickar and Benz 1978; Flewelling and Hubbell 1986). The existence of dipole interactions at the membrane/water interface complicates the interpretation of partition coefficients considerably. This is evident from the above mentioned difference between 2,4-OH-PP and 2,4,6-OH-PP. Contrary to the prediction from bulk phase data, the addition of a hydrophilic OH-group gives rise to a threefold increase of the partition coefficient $\gamma_{m/w}$. This is an effect of the considerably larger value of the contribution, b, to the dipole potential for 2,4,6-OH-PP (see Table 1). Thus the negative energetic effect which is due to the presence of the additional OH-group, is more than compensated for by a positive electrostatic contribution, which is due to a modified dipole moment of the molecule.

In view of the structural and energetic differences between the membrane/water system on the one hand and a bulk phase equilibrium on the other hand, there is no reliable a priori prediction of membrane/water partition coefficients from bulk phase data so far. The development of a theoretical framework for the calculation of permeability data of hydrophobic compounds in biological membranes requires an extensive base of experimental data from lipid membranes.

Acknowledgements. The study has been supported by a scholarship of the Landesgraduiertenförderung Baden-Württemberg to R. A. and by a grant of the Deutsche Forschungsgemeinschaft (Az. Sta 236/1).

References

Andersen OS, Finkelstein A, Katz I, Cass A (1976) Effect of phloretin on the permeability of thin lipid membranes. J Gen Physiol 67:749–771

Awiszus R, Stark G (1988) A laser-T-jump study of the adsorption of dipolar molecules to planar lipid membranes. I. 2,4-Dichlorophenoxyacetic acid. Eur Biophys J 15:299–310

Collander R, Bärlund H (1933) Permeabilitätsstudien an Chara Ceratophylla. II. Die Permeabilität für Nichtelektrolyte. Acta Botan Fenn 11:1–114

Cousin JL, Motais R (1978) Effect of phloretin on chloride permeability: A structure-activity study. Biochim Biophys Acta 507:531–538

DeLevie R, Rangarajan, K, Seelig PF, Andersen OS (1979) On the adsorption of phloretin onto black lipid membrane. Biophys J 25:295–300

Flewelling RF, Hubbell WL (1986) The membrane dipole potential in a total membrane potential model. Biophys J 49: 541–552

Hansch C, Leo A (1979) Substituent constants for correlation analysis in chemistry and biology. J Wiley & Sons, New York

Le Fevre PG (1961) Sugar transport in the red blood cell: structure-activity relationships in substrates and antagonists. Pharmacol Rev 13:39–70

Liberman YeA, Topaly VP (1969) Permeability of bimolecular phospholipid membranes for fat soluble ions. Biophysics 14: 477–487

Lieb WR, Stein WD (1986) Non-Stokesian nature of transverse diffusion within human red cell membranes. J Membr Biol 92:111–119

Macey RI, Farmer REL (1970) Inhibition of water and solute permeability in human red cells. Biochim Biophys Acta 211: 104–106

McLaughlin S (1973) Salicylates and phospholipid bilayer membranes. Nature 243:234–236

Melnik E, Latorre R, Hall JE, Tosteson DC (1977) Phloretin-induced changes in ion transport across lipid bilayer membranes. J Gen Physiol 69:243–257

Pickar AD, Benz R (1978) Transport of oppositely charged lipophilic probe ions in lipid bilayer membranes having various structures. J Membr Biol 44:353–376

Reyes J, Greco F, Motais R, Latorre R (1983) Phloretin and phloretin analogs: Mode of action in planar lipid bilayers and monolayers. J Membr Biol 72:93–103

Szabo G (1976) The influence of dipole potentials on the magnitude and the kinetics of ion transport in lipid bilayer membranes. In: Heinrich MR (ed) Extreme environment: Mechanisms of microbial adaptation. Academic Press, New York, pp 321–348

Verkman AS (1980) The quenching of an intramembrane fluorescent probe. A method to study the binding and permeation of phloretin through bilayers. Biochim Biophys Acta 599: 370–379

Verkman AS, Solomon AK (1980) Kinetics of phloretin binding to phosphatidylcholine vesicle membranes. J Gen Physiol 75: 673–692

Wieth JO, Dalmark M, Gunn RB, Tosteson DC (1973) The transfer of monovalent inorganic anions through the red cell membrane. In: Gerlacher E, Moser K, Deuth E, Wilmanns W (eds) Erythrocytes, thrombocytes, leukocytes. Georg Thieme, Stuttgart, pp 71–76